Journal of
Engineering Sciences
Faculty of Engineering
Assiut University
JES
مجلة
العلوم الهندسية
كلية الهندسة
جامعة أسيوط
journal homepage: http://jesaun.journals.ekb.eg

Prediction of Axial Compressive Strength of Hybrid Reinforced Concrete Columns under Static Loading

Received 5 July 2022; Revised 1 November 2022; Accepted 1 November 2022

Mostafa A. Mohamed[1]
AbdelRahman Megahid[2]
Mohamed M. Ahmed[3]
Omar A. Farghal[4]

Keywords
hybrid CFRP-steel, hybrid GFRP-steel, Columns, Compression.

Abstract

Steel corrosion is thought to be one of the primary causes of the inadequate durability of concrete buildings in the maritime environment. Because of this, adopting Fiber-Reinforced Polymer (FRP) bars in harsh settings has attracted a lot of attention for its appealing mechanical properties as well as to prevent corrosion issues. But because there hasn't been much research in this area, we don't fully understand how fiber-reinforced polymer (FRP) bars behave when they are compressed. This work's goal is to assess the expected axial compressive strength of columns when hybrid reinforcement is used in place of steel reinforcement. Hybrid bars are steel bars surrounded by a cover shell of Glass or Carbon FRP (hybrid-steel) for longitudinal reinforcement and/or transverse reinforcement. 17 column specimens were included in an experimental study program that was created. The specimens were tested to failure with an axial loading condition. The parameters studied were the type of fibers, the percentage of steel in the hybrid reinforcement for longitudinal main reinforcement ρ_L (0.96, 0.44, and 0.25), the ratio of the web reinforcement (internal ties), the proportion of fiber in the hybrid bars, as well as the columns' cross sections' rectangularity. Based on the data, mathematical models were devised and assessed to forecast the load bearing capability of the column. The findings indicate that hybrid reinforced concrete columns have acceptable levels of dependability index in general.

1. Introduction

In reinforced concrete (RC) buildings, corrosion of the steel reinforcement resulted in higher maintenance costs and decreased functioning of structural components. Steel reinforcement may be successfully replaced by fiber-reinforced polymer composites.

[1] Ph. D Candidate, Civil Engineering Dept., Faculty of Engineering, Assiut University, Egypt. mostafaahmedp38@eng.au.edu.eg
[2] Professor, Civil Engineering Dept., Faculty of Engineering, Assiut University, Egypt. abdelrahman.ghonaim@eng.au.edu.eg
[3] Professor, Civil Engineering Dept., Faculty of Engineering, Assiut University, Egypt. mohamed.mohamed33@eng.au.edu.eg
[4] Professor, Civil Engineering Dept., Faculty of Engineering, Assiut University, Egypt. oahmed@eng.au.edu.eg

https://doi.org/10.21608/JESAUN.2022.149280.1153

Although FRP bars are regarded as light weight, high strength, and durable enough to replace steel bars, their use is still restricted, particularly in members of compression. Some reasons are that the FRP bar has, in general, a low elastic modulus and the anisotropic nature of FRP. In addition, the various types of failure for specimens under compression load impact how FRP bars respond to compression (shear failure, buckled GFRP bar, and transverse tensile failure); hence suitable design principles are required.

Due to the lack of experimental data, FRP bars in compression members must be established to get widespread acceptability from engineers. However, the ACI 440.1R-06[1] design guidelines still do not recommend using glass-fiber-reinforced polymer (GFRP) bars are used in compression members as longitudinal reinforcement. ACI 440.1R-15[2] emphasizes the necessity for more study on columns reinforced with fiber bars.

Canadian regulations state that GFRP reinforcement cannot be considered as providing compressive resistance when used as compression reinforcement in flexural components or longitudinal reinforcement in columns[3]. The analysis of the compression characteristics of FRP bars serves as the starting point for the study on FRP-RC members of compression. Numerous experimental tests show that the FRP bars' maximal tensile strength is equivalent to 20–70% of their ultimate compressive strength. Additionally, the tensile elastic modulus and the compressive elastic modulus have a basic similarity. (Guowei Ma et al., [4]; Laith AlNajmi and Farid Abed, [5]. Longitudinal FRP bars significantly impact the effectiveness of FRP-RC columns in axial compression. Previous research revealed the axial load-carrying capacity capability of CFRP-RC columns for the same longitudinal reinforcement ratio is 12–16 % smaller than that of RC columns reinforced with steel. The steel bars' load contributes to approximately 11 percent -16 percent of the overall load borne by RC columns. At the same time, GFRP bars made of glass-fiber reinforced polymer contribute about 3–10% of the about 3–10% of the maximum load. Afifi, [6]; Alsayed et al., [7]; Mohamed et al., [8]; Pantelides et al., [9]; Tobbi et al., [10], [11]; GFRP bars are more prone to buckling failure than steel bars because of their low elastic modulus. Additionally, GFRP stirrup bars tend to confine to concrete less than steel stirrup bars of the same volumetric ratio. Brown et al., [12]; De Luca et al., [13]. As a result, For GFRP-RC columns, the stirrup's design is crucial. Mohamed et al. [8], Twelve circular reinforced concrete (RC) columns tested for axial loads at full scale were assessed. The columns were reinforced using longitudinal glass FRP (GFRP) bars and newly manufactured GFRP spirals. The test findings showed that the behavior of the GFRP and steel RC columns was comparable. The longitudinal GFRP bars' average load carried ranged from 5–10% of the maximum load. Instead of employing larger diameters with broader spacing, smaller-diameter GFRP spirals with tighter spacing may boost ductility and confinement efficiency. The maximum capacity of the tested specimens was underestimated by leaving out GFRP bars from the design equation. To improve the confinement on the concrete The volumetric ratio of a GFRP-RC column with square sections may be enhanced by modifying transverse reinforcement configuration, material type, and spacing to create a confined concrete zone. Tobbi et al., [10], [11] or casting concrete around the reinforcing sections Hadi and Youssef,(2016)[14]; Hadhood A, et al., [15]). Omar Ahmed Farghal al. [16] investigated the gain strength of reinforced concrete (RC) columns included with CFRP sheets using Eighteen circular short column specimens were evaluated under axial compression. The CFRP sheets' volume and configurations, the cross-section's size, the proportion of main reinforcement, and the internal stirrups' volume were the variables examined. Based on the

obtained results, mathematical models of (Egyptian code[17],[18] and American Concrete Institute code[1], [2]) The suggested method for predicting the axial compressive strength of a non-slender RC column reinforced with CFRP sheets is assessed. As a result, modifications to the models in the study were taken into consideration. The modifications account for the lateral confining pressure caused by internal steel stirrups.

The modified code equations demonstrated a respectable approach to dealing with the study results. Haytham F. Isleem et al. [19] Examined The stress-strain response of square concrete columns constrained by internal GFRP hoops and subjected to axial compression loading is predicted using a closed-form formula. The test findings were not adequately predicted by existing models for concrete with a circular cross-section contained by FRP hoops or concrete confined by steel. The model also considers the impacts of the longitudinal bar type, volumetric ratio, size, arrangement, and spacing of the reinforcing hoop (i.e., steel as opposed to GFRP).

As previously stated, design guidelines don't include FRP reinforced columns or reliability-based calibration provisions. A generic design process for rectangular (hybrid-steel) reinforced columns under concentric load is thus presented in this paper. Seventeen columns under concentric loads were used in the experiments that formed the basis for the design process and dependability study.

2. Research significance.

Currently, The Canadian standards only CSA A23.3[20] and S6 [21] Include FRP-RC column design considerations, even for seismic loads. Other design standards, however, neglect the contribution of FRP bars to compression and don't provide any design codes for FRP reinforced concrete columns. As a consequence, this study will assess researchers who modified the design requirements of ACI-440[1], [2]and EC [17], [18] by offering design recommendations based on reliability analysis to gauge the degree of safety. The outcome demonstrates that including the compressive contribution of (fiber-encased steel bars) would provide findings with a degree of safety that is acceptable and more accurate.

3. Database and Experimental Results

3.1. Materials

The material properties used to produce the columns are as follows:

3.1.1 Concrete

All columns have been cast by using a concrete mix of ordinary Portland cement, sand, and coarse aggregate of crushed dolomite, with 10mm maximum nominal size, and water with ratios of 1: 2: 4: 0.5 by weight respectively. The dry sand, gravel, and cement are mixed mechanically for one minute to ensure the uniformity of the mix. The water is then added to the dry materials, and the contents are mechanically mixed for about three minutes. Where the properties of the used materials and their matches with ECP203.

3.1.2 Steel Reinforcement

Smooth, mild steel 8mm diameter bars were used for stirrups(B240C-P), while 12mm diameter deformed steel bars(B420DWR) and hybrid-steel were used for vertical or

transverse reinforcement. Hybrid bar fabrication consists of steel, fiber rolls (E-glassfiber2400) or CFRP fabric type (sika wrap® -230C) as yarns fiber, resin polyester, Vinylester, and epoxy resins. See Fig. (1).

A total of 20 specimens of 550 mm in length were prepared and tested in tension according to ECG 208-2005[17], as shown in Fig (2). All specimens were fixed at the top and bottom with a steel grip of 220mm long steel tubes, filling an epoxy material, see Fig. (3). The specimens were kept more than 30 days before testing to allow curing. The loads were applied to the specimens by a 100(KN) capacity testing machine. The failure mode of the hybrid bars is shown in Fig. (4). Tables (1) to (3) provide information on the characteristics of the reinforcing bars utilized in the tested columns.

Fig.(1): Reinforcement hybrid -steel bars

Fig.2: Tensile test setup.

Table 1: Properties of the steel reinforcement.

Bar diameter (mm)	Actual diameter (mm)	Yield Stress (MPa)	Ultimate stress (MPa)	Modulus of elasticity (GPa)	Elongation %
8	8	360	420	200	18
10	11.5	490	655	200	20

Fig.3: preparing bars to tested.

Fig.4: Failure of the hybrid-steel bars tensile test specimen.

Table 2: Properties of the hybrid reinforcement.

Hybrid Bar diameter (mm)	Actual diameter (mm)	Type of hybrid	Yield Stress (MPa)	Ultimate stress (MPa)	Tensile modulus of elasticity (GPa.)	Elongation %
6/6G/12	11.8	Steel – glass	360	522.5	124	1.34
8/4G/12	11.8		385	701.0	132	1.45
10/2G/12	11.8		400	862.2	139	1.65
6/6C/12	11.8	Steel – Carbon	385	522.5	135	1.22
8/4C/12	11.8		405	701.0	158	1.28
10/2C/12	11.8		445	862.2	168	1.42

Note: a/bx/d; a = steel bar diameter , b = thickness of fiber shell, x= type of fiber and d= overall hybrid bar diameter

Table 3: Properties of the FRP bars

Fiber Bar diameter (mm)	Actual diameter (mm)	Type of fiber bars	Tensile strength, MPa	Tensile modulus of elasticity, GPa	Ultimate strain%
12	11.8	glass	1100	60	2.55
12	11.8	Carbon	2050	145	1.45

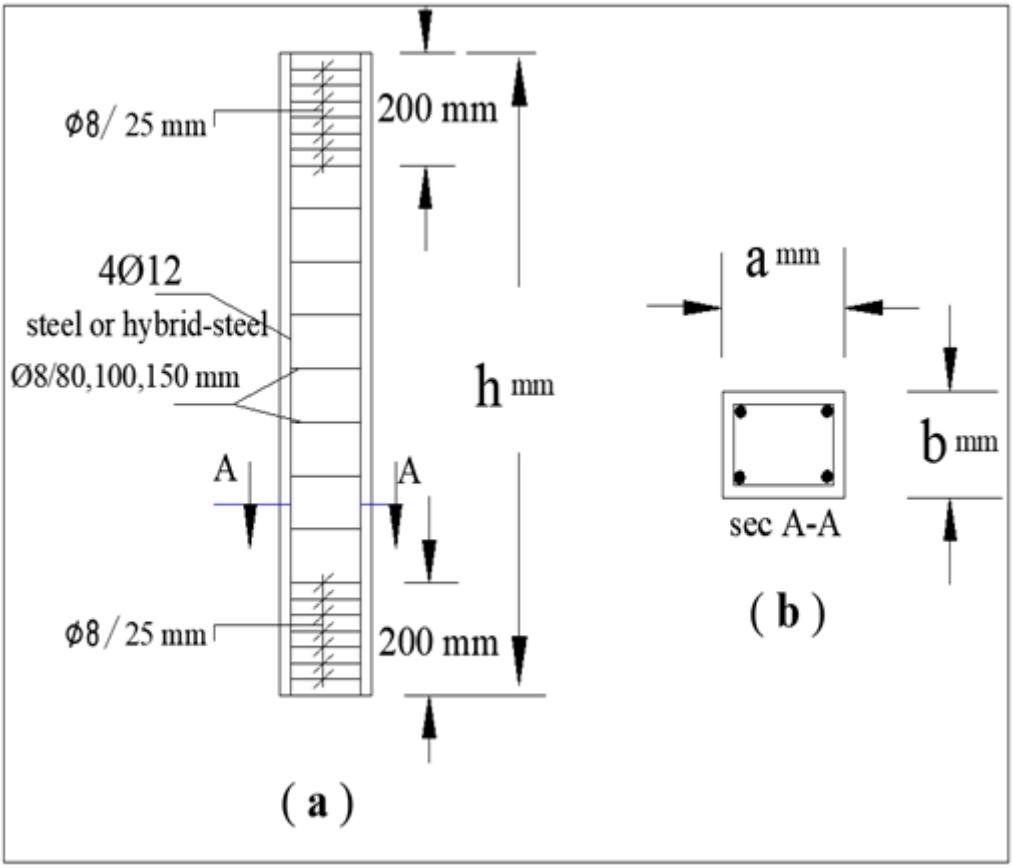

Fig. 5: Typical details of the tested columns

3.2 Layout of experiments:

The author carried out an experimental program including 17 RC columns, as shown in Fig (5), Fig (6) and Table (4). The specimen was kept more than 30 days before testing to allow curing. At a concrete age of 28 days, all columns were tested. Group Specimens' Details as below:

- For group A, as a reference column, Column C1 was reinforced using longitudinal steel reinforcement, and the other columns were reinforced with hybrid bars, as illustrated in Table (4). All examined columns' end zones were equipped with closed stirrups placed 200mm apart and at a 25mm interval. Four (glass fiber-encased steel bars) with a total diameter of 12 mm were used as longitudinal reinforcement for Columns C2, C3, and C4. In the form of inner steel bars core (Ø6, Ø8, Ø10mm), surrounded by a shell cover of glass fiber polymer, the transverse reinforcement was steel bars with 8 mm diameter; see Fig. (7) and Table. (4). Column C5 was reinforced with a four 12-mm diameter GFRP bars.
- In group B, Columns C6 and C7 were identical to columns C2, but had concrete compressive strengths of 35.6 and 44.9 MPa, respectively.
- Columns C8 and C9 for group C were identical to column C2 but with stirrup spacing of 80 mm and 150 mm, respectively.
- In group D, columns C10 and C11 were reinforced similarly to column C2, with the volumetric ratio of the glass fiber shells being 85% and 75%, respectively, to match column C2.
- 5) Group E, Columns C12 and C13, were made of sections of 260 mm by 150 mm and 235 mm by 170 mm, respectively, and were reinforced with four 12 mm hybrid GFRP-steel bars.

- 6) For group F, four 12-mm CFRP bars strengthen column C14. The remaining columns, C15, C16, and C17, were strengthened with four bars of total diameter 12 mm as longitudinal reinforcement in the form of inner steel bars core (6, 8, 10mm). The utilized steel bars were covered with a Carbone fiber polymer coating (carbon fiber-encased steel bars).

Axial compressive loads were applied to the column specimens by using a universal testing machine of 5000 KN capacity, as shown in Fig (8). The compressive failure load from the experimental test was studied and analyzed elsewhere [22], included in Table. (5).

Table 4: Details of the tested columns:

Group No	Column NO.	Height(mm)	Cross section (mm)	Longitudinal Reinforcement				Web Reinforcement (Internal ties)			Concrete compressive strength f_c N/mm^2	cylindrical axial compressive strength predicts f_c' N/mm^2
				steel	hybrid	% Of Fiber	ρ_L	steel	hybrid	μ		
A	C1	1200	200×200	4Φ12	-		1.00	Ø8/120mm	-	0.004	24.5	19.60
	C2			-	4Φ10/2G/12	100	0.96	Ø8/120mm	-	0.004	24.5	19.60
	C3			-	4Φ8/4G/12	100	0.44	Ø8/120mm	-	0.004	24.5	19.60
	C4			-	4Φ6/6G/12	100	0.25	Ø8/120mm	-	0.004	24.5	19.60
	C5			4Φ12 GFRP-bar		100	0.0	Ø8/120mm	-	0.004	24.5	19.60
B	C6	1200	200×200	-	4Φ10/2G/12	100	0.96	Ø8/120mm	-	0.004	35.6	28.48
	C7			-	4Φ10/2G/12	100	0.96	Ø8/120mm	-	0.004	44.9	35.92
C	C8	1200	200×200	-	4Φ10/2G/12	100	0.96	Ø8/80mm	-	0.006	24.5	19.60
	C9			-	4Φ10/2G/12	100	0.96	Ø8/150mm	-	0.003	24.5	19.60
D	C10	1200	200×200	-	4Φ10/2G/12	85	0.96	Ø8/120mm	-	0.004	24.5	19.60
	C11			-	4Φ10/2G/12	75	0.96	Ø8/120mm	-	0.004	24.5	19.60
E	C12	1002	235×170	-	4Φ10/2G/12	100	0.96	Ø8/120mm	-	0.004	24.5	19.60
	C13	900	260×150	-	4Φ10/2G/12	100	0.96	Ø8/120mm	-	0.005	24.5	19.60
F	C14	1200	200×200	4Φ12CFRP-bar		100	0.0	-	Ø6/2G/8/120mm	0.004	24.5	19.60
	C15			-	4Φ10/2C/12	100	0.96	-	Ø6/2G/8/120mm	0.004	24.5	19.60
	C16			-	4Φ8/4C/12	100	0.44	-	Ø6/2G/8/120mm	0.004	24.5	19.60
	C17			-	4Φ6/6C/12	100	0.25	-	Ø6/2G/8/120mm	0.004	24.5	19.60

f_c *is the compressive strength of a standard cube 150x150x150mm*

ρ_L *= Ratio of steel to (GFRP or CFRP) in the reinforced bar=* $(A_{steel}/ (A_{steel} + A_{fiber})$

μ*= Ratio of the web reinforcement (internal ties) =* $\frac{n\,At}{S.b}$

scale category of the tested columns: one-third

Fig. (6): preparing Cages of Column

Fig. (7): Cages of Columns

Fig. 8: Testing of column specimens

4. Results and Discussion:

Table (5) presents the experimental results of various specimens. The testing results showed that hybrid reinforced columns' axial strength was (9 - 5%) higher than their reference column.

Table (5): Results of the tested columns:

Group No	Column No.	Cracking load (KN)	Ultimate load (KN)	Failure mode
A	C1	680	885	Comp-failure
	C2	830	940	Comp-failure
	C3	780	905	Comp-failure
	C4	735	882	Comp-failure
	C5	710	833	Comp-failure
B	C6	1100	1210	Comp-failure
	C7	1200	1345	Comp-failure
C	C8	850	915	Comp-failure
	C9	780	853	Comp-failure
D	C10	750	880	Comp-failure
	C11	730	865	Comp-failure
E	C12	790	890	Comp-failure
	C13	755	875	Comp-failure
F	C14	680	781	Comp-failure
	C15	890	963	Comp-failure
	C16	788	898	Comp-failure
	C17	765	890	Comp-failure

4.1 Failure Modes

Fig. (9) shows the examined specimens' failure mechanisms. Following the application of the load, the concentrically loaded columns exhibited elastic behavior up to around 80–90% of the maximum axial strength. There were no visible cracks in the concrete cover currently. When the load was increased further, the little vertical hairline fractures on the compression side of the columns were triggered, which caused the concrete cover to crack and produce a faint sound. Therefore, as the load grew, so did the number of cracks. At the conclusion of this phase, the hybrid steel will suddenly and explosively fracture, the longitudinal hybrid GFRP-steel bars will rupture and buckle, and the concrete core will eventually be crushed. The rupture was comparatively more sudden and explosive in the columns reinforced with hybrid GFRP-steel bars than in the specimen reinforced with steel bars.

Fig. 9: Failure overview for specimen

4.2 Nominal axial capacity

By assuming the concrete and steel's contribution to compression, it is possible to calculate the nominal axial capacity of short columns that are concentrically loaded and strengthened by longitudinal steel bars. According to either the ACI or Canadian codes, the column capacity, and the yielded steel bars (i.e., $\varepsilon_{steel} \geq 0.002$) in the ultimate limit state may be calculated as provided in Eqs. (1) and (2), respectively. It is recommended to exclude the contribution of FRP reinforcement in compression, according to the CAN/CSA S806 [3]

and ACI-440[2]. The nominal axial capacity of FRP-RC columns may be calculated using the formula provided in Eq. (2) based on this advice. Where P_n is the nominal axial capacity; A_g is the columns' gross area; A_f is the area of FRP bars.

$$P_n = 0.85f'_c (A_g - A_s) + A_s f_y \quad \text{Eq. (1).}$$

$$P_n = 0.85f'_c (A_g - Af) \quad \text{Eq. (2).}$$

In the reviewed literature, several researchers proposed several methods for adding the FRP impact in nominal axial capacity; however, there was no information on methods for columns strengthened with hybrid bars.
The method assumes a linear stress-strain relationship to determine the stress in the FRP bars. (*i.e.*, $\sigma_{FRP} = E_f \times \varepsilon$), E_f is the FRP bars' elastic modulus and limiting the strain ε to 0.002 (Eq. (3)).

$$P_n = 0.85f'_c (A_g - A_f) + 0.002E_f A_f \quad \text{Eq.(3).}$$

This work believed that the modified models (ACI[1], [2], ECs[17], [18], Afifi[6], Tobbi[11], and Mohamed, H.M Afifi[8]) would predict the maximum nominal compressive strength (P_n) of hybrid RC column specimens as listed in Table (6). The nominal axial loads *Pn* is predicted according to these modified models and were listed in Tab. (7).

Table 6: Various axial capacity models for evaluation

Capacity mode	The relationship for capacity model	Model modifications
ACI-318–08	$P_n = 0.85f'c\ (Ag - A_f) + f_y A_s$	$P_n = 0.85f'_c(A_g - A_h) + f_h A_h$
ECs	$P_n = 0.9[0.8X0.85f_c (A_g - A_f) + f_y A_f$	$P_n = 0.9[0.8X0.85f_c(A_g - Ah) + f_h A_h$
Afifi et al.	$P_n = 0.85f'_c(A_g - A_f) + .002E_f A_f$	$P_n = 0.85f'_c(A_g - A_h) + .002EhAh$
Mohamed et al.	$P_n = 0.85f'_c(A_g - Af) + 0.35f_f A_f$	$P_n = 0.85f'c(A_g - A_h) + 0.35f_h Ah$
Tobbi et al.	$P_n = 0.85f'_c(A_g - A_f) + .003E_f A_f$	$P_n = 0.85f'c(A_g - A_h) + .003E_h A_h$
Current study	$P_n = 0.85f'_c(A_g - A_h) + 0.30f_h A_h$	

(Hybrid –Steel) =FRP and Steel

Where P_n is the nominal axial capacity, A_g is the columns' gross area; A_h, f_h and E_h are the total area, yield stress, and the elastic modulus of the longitudinal reinforcement (hybrid – steel), respectively, and f_c is the concrete strength.

4.3 Axial Strength Model

According to the selected modified models (ACI[1], [2], ECs[17], [18], Afifi[6], Tobbi[11], Mohamed, H.M Afifi[8], and present study) the maximum compressive strength P_n of hybrid reinforced concrete columns was determined and is shown in Table 5. Table 6 shows comparisons between computed values of (P_n) and those obtained from experimental data found in the literature study. This would be determined by looking at the average value, standard deviation, and correlation factor for each of the estimated values in Table 7. Finally, the models predict the nominal axial load of hybrid steel and reinforced concrete (RC) columns more precisely. The different proposed models showed an acceptable approach to the experimental results particularly those proposed by modified Egyptian code (EC) and modified ACI code.

Table 7: Analytical verification of maximum loads for the tested columns:

Group No	Column No.	$P_{max.}$	Prediction results											
			Modified Egyptian code (EC)		Modified ACI cod		Modified Afifi et al.		Modified Mohamed, H.M Afifi et al.		Modified Tobbi et al.		Current study	
			P_n (KN)	R_{max} (%)	P_n (KN)	R_{max} (%)	P_n (KN)	R_{max} (%)	P_n (KN)	R_{max} (%)	P_n (KN)	R_{max} (%)	P_n (KN)	R_{max} (%)
A	C1	885	739.43	96.10	880.35	99.47	659.05	74.47	736.39	83.21	659.14	74.48	725.31	81.96
	C2	940	755.70	89.89	884.87	94.14	659.00	70.11	737.97	78.51	823.78	87.64	726.67	77.31
	C3	905	749.60	92.02	878.09	97.03	658.99	72.82	735.60	81.28	823.77	91.02	724.64	80.07
	C4	882	739.43	94.87	866.79	98.28	658.98	74.71	731.64	82.95	823.76	93.40	721.25	81.77
	C5	833	721.12	104.34	708.59	85.06	658.92	79.10	676.27	81.19	823.67	98.88	673.79	80.89
B	C6	1210	1024.36	96.24	1183.38	97.80	957.50	79.13	1036.48	85.66	1196.91	98.92	1025.18	84.73
	C7	1345	1249.45	105.04	1433.48	106.58	1207.61	89.78	1286.58	95.66	1509.54	112.23	1275.28	94.82
C	C8	915	755.70	91.52	884.87	96.71	659.00	72.02	737.97	80.65	823.78	90.03	726.67	79.42
	C9	853	755.70	98.95	884.87	103.74	659.00	77.26	737.97	86.51	823.78	96.57	726.67	85.19
D	C10	880	745.53	104.63	873.57	99.27	658.99	74.88	734.01	83.41	823.76	93.61	723.28	82.19
	C11	865	727.23	106.60	853.23	98.64	658.98	76.18	726.90	84.03	823.76	95.23	717.18	82.91
E	C12	890	755.70	94.38	868.21	97.55	642.34	72.17	721.31	81.05	802.95	90.22	710.01	79.78
	C13	875	755.70	96.18	884.04	101.03	658.16	75.22	737.14	84.24	822.73	94.03	725.84	82.95
F	C14	781	733.33	93.90	751.53	96.23	659.00	84.38	691.30	88.51	823.78	105.48	686.67	87.92
	C15	963	774.01	89.79	893.91	92.83	659.02	68.43	741.13	76.96	823.81	85.55	729.38	75.74
	C16	898	757.74	91.43	887.13	98.79	659.01	73.39	738.76	82.27	823.80	91.74	727.35	81.00
	C17	890	749.60	93.16	860.01	96.63	658.99	74.04	729.27	81.94	823.77	92.56	719.21	80.81
Average (%)			97.07		97.63		75.77		83.41		93.62		82.32	
Stander deviation			5.71		4.58		5.18		4.21		7.89		4.31	
Correlation factor R^2			0.93		0.97		0.95		0.97		0.93		0.97	

R_{max}: the ratio of predicted maximum load to that obtained experimentally 'P_n/P_{max}'

4.4 Validation of the models' proposals

Given the background, the improved models proposed in this study's predictions for the load-carrying capacity of reinforced concrete columns utilizing hybrid steel exhibited a superior estimate that was closer to the experimental data, see Table (6)and Fig (10). The percentage of the load carrying capacity of hybrid-steel reinforced concrete columns predicted according to the modified models to that obtained experimentally R_{max} *(=P_n/P_{max})* ranged from 89.79% to 98.95% in the case of modified EC and ranged from 85.06% to 98.79% also in case of modified ACI code. For Afifi et al, modified model, R_{max} *(=P_n/P_{max})*

ranged from 68.43% to 89.78% and ranged from 76.98% to 88.51%. also, in the case of the modified model, Mohamed et al. for Tobbi et al; modified model R_{max} $(=P_n/P_{max})$ ranged from 74.48% to 98.88% and ranged from 75.74% to 94.82% also in the case of the current study model. Or, to put it another way, the correlation factor increased to 0.93, 0.97, 0.95, 0.97, 0.93, and 0.97 in the case of modified EC code, ACI code, Afifi, Mohamed, Tobbi, and current study model, respectively. It is noteworthy to point out that the adjusted models provided in this research demonstrated a reasonable estimate approaching the experimental data, particularly in the case of Mohamed et al. modified model with average R_{max}=83.41%, Stander deviation=4.21, and Correlation factor R^2=0.97, see Table. (7)and Fig. (10).

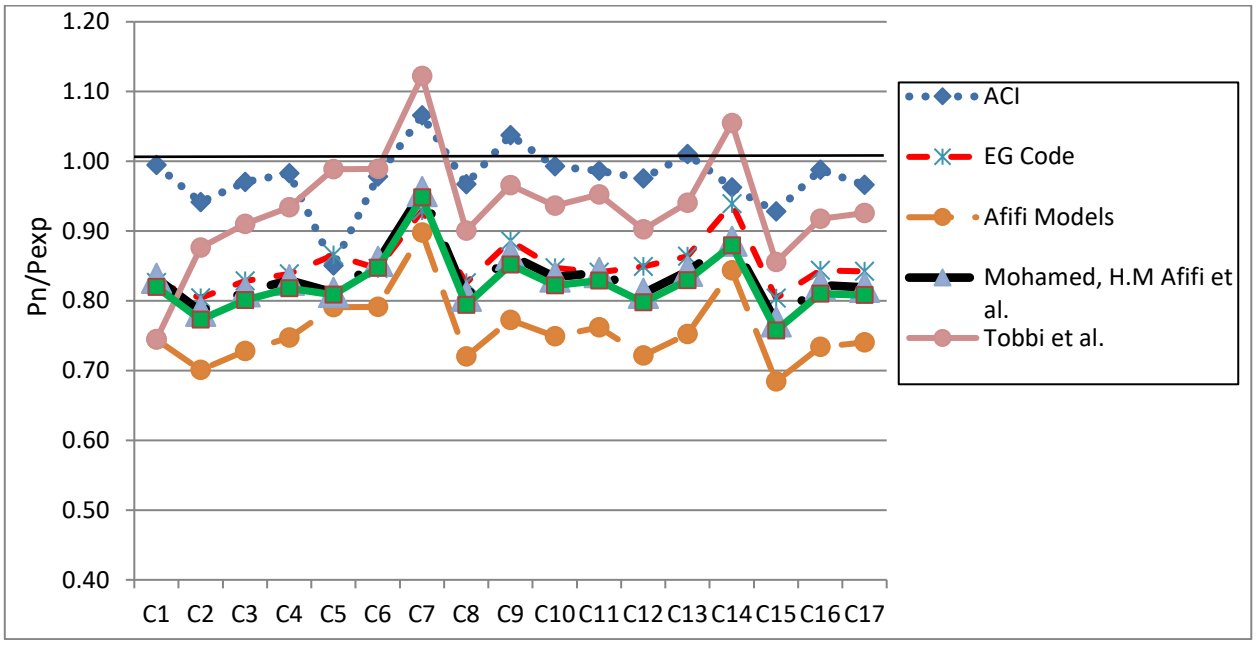

Fig. 10: Predicted-to-experimental ratio of maximum load (P_n/P_{max}) for the various columns

5. Conclusions

The following major conclusions can be drawn from the experimental study on the strain and the available database on the behavior of new hybrid-reinforced concrete columns reinforced with longitudinal reinforcement in the form of an inner steel bar core surrounded by a cover of fiber polymer (hybrid FRP-steel) under concentric loading:

1. Compared to the produced database of 17 specimens, the proposed empirical modified model (ACI, EG, Afifi, Mohamed, H.M. Afifi, and the present study) for predicting the axial load-carrying capacity of hybrid-reinforced columns performed better. This performance attests to its applicability and accuracy.
2. For the study's instance, adjustments to the fiber type, cross-sectional shape, volume of internal ties, and percentage of longitudinal reinforcement had no effect on the dependability index.
3. The dependability index did, however, show some little variations in the strength of the concrete. The nominal capacity of the tested (hybrid FRP-steel) RC columns was accurately and conservatively predicted using a 0.30 reduction factor for the model (present work) to account for the decrease in the compressive strength of the (hybrid FRP-steel) bars as a function of their tensile strength. More experimental data and future investigation are needed. However, it is crucial to detail the compressive properties of (hybrid FRP-steel) bars and considers the effect of column size.

4. A comparison of the suggested empirical model's predictions with the maximum load that 17 hybrid steel reinforced columns can support axially. With an average R_{max} of 83.41, a standard deviation of 4.21, and a correlation coefficient of 0.97, Mohamed et al. modified model's proposed empirical equation for the predicted axial load bearing capacity was confirmed to be accurate.

6.References

[1] A. C. 440:, "ACI Committee 440: Guide for the Design and Construction of Externally Bonded FRP Systems for Strengthening Concrete Structures (ACI 440.2R-02); American Concrete Institute: Farmington Hills, MI, USA, 2008; p. 76.," 2008.

[2] ACI Committee 440, *Guide for the Design and Construction of Structural Concrete Reinforced with Fiber-Reinforced Polymer Bars (ACI 440.1R-15). American Concrete Institute*. 2015.

[3] Canadian Standards Association, *Canadian Standards Association Canadian Highway Bridge Design Code. CSA Code CAN/CSA-S6-06*. 2006.

[4] G. Ma, Y. Huang, F. Aslani, and T. Kim, "Tensile and bonding behaviours of hybridized BFRP–steel bars as concrete reinforcement," *Constr. Build. Mater.*, vol. 201, pp. 62–71, 2019, doi: 10.1016/j.conbuildmat.2018.12.196.

[5] L. Alnajmi and F. Abed, "Evaluation of FRP bars under compression and their performance in RC columns," *Materials (Basel).*, vol. 13, no. 20, pp. 1–19, 2020, doi: 10.3390/ma13204541.

[6] M. M. . Z. M. . Afifi, "BEHAVIOR OF CIRCULAR CONCRETE COLUMNS REINFORCED WITH FRP BARS AND STIRRUPS," 2013.

[7] and A. Alsayed SH, Al-Salloum YA, Almusallam T H and MA, "Concrete columns reinforced by GFRP rod," *4th Int. Symp. Fiber-Reinforced Polym. Reinf. Reinf. Concr. Struct. SP-188. C. W. Dolan SH Rizkalla A Nanni (eds), 8 January, pp. 103–112. Farmingt. Hills, MI Am. Concr. Inst.*, 1999.

[8] B. Afifi, Mohammad Z.Mohamed, Hamdy M.Benmokrane, "Axial Capacity of Circular Concrete Columns Reinforced with GFRP Bars and Spirals," *J. Compos. Constr.*, vol. 18, no. 1, p. 04013017, 2014, doi: 10.1061/(asce)cc.1943-5614.0000438.

[9] R. L. Pantelides CP, Gibbons ME, "Axial load behavior of concrete columns confined with GFRP spirals," *Constr, Compos*, vol. 17, no. 3, 2013.

[10] and B. B. Tobbi, H., Farghaly A. S., "'Concrete Columns Reinforced Longitudinally and Transversally with Glass Fiber-Reinforced Polymers Bars.' AC I Structural Journal, 109 (4), 1-8.," 2012.

[11] B. Tobbi, H.; Farghaly, A.S.; Benmokrane, "Behavior of concentri_cally loaded fiber-reinforced polymer reinforced concrete columns with varying reinforcement types and ratios," *ACI Struct. J. 111(2), 04016109*, vol. 111, no. 2, 2014.

[12] Brown J, "The study of FRP strengthening of concrete structures to increase the serviceable design life in 1564 Advances in Structural Engineering 22(7) corrosive environments," *Res. Report, Univ. West. Aust. Perth, WA, Aust.*, 2012.

[13] A. De Luca, F. Matta, and A. Nanni, "Behavior of full-scale glass fiber-reinforced polymer reinforced concrete columns under axial load," *ACI Struct. J.*, vol. 107, no. 5, pp. 589–596, 2010, doi: 10.14359/51663912.

[14] J. Hadi, M.N.S., Youssef, "Experimental Investigation of GFRP-Reinforced and GFRP-Encased Square Concrete Specimens under Axial and Eccentric Load, and Four-Point Bending Test," *J. Compos. Constr.*, vol. Volume 20, no. Issue 5, 2016.

[15] B. B. Hadhood A, Mohamed HM, "Axial Load-Moment Interaction Diagram of Circular Concrete Columns Reinforced with CFRP Bars and Spirals: Experimental and Theoretical Investigations. J Compos Construct, ASCE 2017;21 (2):04016092. https://doi.org/10.1061/(ASCE)CC.1943-5614.0000748.," 2017.

[16] O. A. Farghal and H. M. A. Diab, "Prediction of axial compressive strength of reinforced concrete circular short columns confined with carbon fiber reinforced polymer wrapping sheets," *J. Reinf. Plast. Compos.*, vol. 32, no. 19, pp. 1406–1418, 2013, doi: 10.1177/0731684413499830.

[17] E. code for design principals and construc tion specifications of using F. system for Construction., F. and Egypt: Ministry of Housing, N. C. for Constructional Development, and 2005. Housing and Construction Research, *EC 208*. 2005.

[18] ECP203, *ECP203-2020*. .

[19] Haytham F. Isleem Daiyu Wang Zhenyu Wang, "Axial stress–strain model for square concrete columns internally confined with GFRP hoops," *Mag. Concr. Res.*, vol. 70, no. 20, pp. 1064–1079, 2018.

[20] CSA, *CSA A23.3:19 Design of concrete structures*. 2019.

[21] CSA, *CSA S6 - Canadian highway bridge design code*. 2017.

[22] M. M. A. and O. A. F. Mostafa Ahmed Mohamed, Abd El-Rahman Megahid Ahmed, "STRUCTURAL BEHAVIOROF HYBRID. REINFORCED COLUMNSUNDER STATIC LOADING." *Recent Applications and Future Challenges International Conferences(ICCE2021*. Hurghada, Egypt.

التنبؤ بقدرة التحمل للأعمدة الخرسانية المسلحة بتسليح هجين المختبرة تحت تأثير حمل محوري

الملخص العربي

تآكل وصدأ الحديد هو أحد الأسباب الرئيسية لتدهور المباني الخرسانية وخاصة في البيئة البحرية. ولهذا السبب، فإن تبني استخدام قضبان البوليمرات المقواه بالألياف (FRP) في البيئات العدوانية قد جذبت الكثير من الاهتمام لخصائصها الميكانيكية الجذابة وكذلك لمنع مشاكل التآكل وصدأ الحديد. ولكن نظرًا لأنه لم يكن هناك الكثير من الأبحاث في هذا المجال، فإننا لا نفهم تمامًا كيف تتصرف قضبان البوليمرات المقواه بالألياف (FRP) عند تعريضها لقوي ضغط.

وعليه فإن هدف هذا العمل هو حساب وتقييم قوة الضغط المحورية المتوقعة للأعمدة عند تسليحها باستخدام قضبان التسليح الهجين بدلاً من تسليح الصلب أو قضبان البوليمرات المقواه بالألياف.

القضبان الهجينة المستخدمة في هذا البحث هي عبارة عن قضبان فولاذية محاطة بغطاء من بوليمرات الياف الزجاج أو الكربون (الصلب الهجين) من أجل استخدامها كتسليح طولي او تسليح الكانات.

في هذه الدراسة تم اختبار ١٧ عينة عمود في برنامج تجريبي. تم اختبار العينات حتى الانهيار تحت تأثير حمل محوري. كانت المتغيرات التي تم دراستها هي] نوع الألياف، النسبة المئوية للصلب الهجين للتسليح الرئيسي الطولي ρ_L(0.96, 0.44, 0.25)، نسبة تقوية العصب "كانات التسليح الداخلية"، ونسبة الألياف في القضبان الهجينة، وكذلك نسبة المستطيلة للمقاطع العرضية المستطيلة للأعمدة] . واستنادًا إلى تلك البيانات، تم اختيار بعض النماذج الرياضية وتقييمها للتنبؤ بقدرة التحمل للأعمدة المسلحة بهذا التسليح الهجين. وقد اثبتت الدراسة ان النماذج الرياضية المقترحة للتنبؤ بقدرة حمل الاعمدة المسلحة بتسليح هجين تقارب النتائج التي تم الحصول عليها معمليا وبخاصة النماذج المقترحة من الكود الامريكي ومحمد عفيفي واخرين.